Pattern Selection and Spatiotemporal Transition to Chaos in the Ginzburg-Landau Equation

K. Nozaki and N. Bekki
Department of Physics, Nagoya University, Nagoya 464, Japan
(Received 5 August 1983)

It is shown that a modulationally unstable pattern is selected and propagates into an initially unstable motionless state in the one-dimensional generalized Ginzburg-Landau equation. A further spatiotemporal transition occurs with a sharp interface from the selected unstable pattern to a stabilized pattern or a chaotic state. The distinct transition makes a coherent structure coexist with a chaotic state.

PACS numbers: 03.40.Kf, 05.70.Ln

A coherent structure and a chaotic state are two distinct states of nonlinear dissipative wave systems. In this Letter, we investigate spatiotemporal transitions from an unstable motionless state to a coherently oscillating state and a chaotic state. As a model equation describing such phenomena as generally as possible, we take the generalized time-dependent Ginzburg-Landau equation:

$$i\psi_t + p\psi_{xx} + q|\psi|^2\psi = i\gamma\psi, \tag{1}$$

where $p = p_r + ip_i$ and $q = q_r + iq_i$ and we assume that $|p_r| = |q_r| = 1$, $p_i < 0$, $q_i > 0$, and $\gamma > 0$. This equation has a quite wide range of applications such as a phase transition in nonequilibrium systems,[1] Bénard convection,[2] Taylor-Couette flow,[3] plane Poiseuille flow[4] in fluid systems, drift dissipative waves in plasma physics,[5] chemical turbulence,[6] and ionization waves in the glow discharge.[7] The following three different states are well-known solutions of Eq. (1): a motionless state ($\psi = 0$), periodic patterns described by finite-amplitude plane-wave solutions, and chaotic states.[6,8] The crucial question is how and under what condition a localized initial disturbance grows up into a periodic pattern and a chaotic state. A striking result of our investigation is the occurrence of a sharp selection of a modulationally unstable pattern although many other stable patterns are possible when $p_r q_r + p_i q_i < 0$. Even in the case $p_r q_r + p_i q_i > 0$ where any equilibrium patterns (finite-amplitude plane-wave solutions) become unstable for long-wavelength perturbations, a selected periodic pattern can propagate in the motionless state, accompanying a chaotic region. As a result of this, the coexistence of a coherent state and a chaotic state occurs with a sharp interface.

(1) The transition from a quiescent state to a periodic pattern can be described by a shock solution:

$$\psi = \psi_0 e^{i(Kx - \Omega t)}\tilde{\psi}(x - vt), \tag{2}$$

$$\Omega = p_r K^2 - q_r|\psi_0|^2, \quad |\psi_0|^2 = (\gamma + p_i K^2)/q_i, \tag{3}$$

where K and v are chosen so that $|\tilde{\psi}|$ vanishes at one infinity and approaches 1 at the other infinity. It may be instructive to show the following explicit solution which assures the existence of such K and v:

$$\tilde{\psi} = \{1 + e^{\kappa(x - vt)}\}^{-(1+i\alpha)}, \tag{4}$$

$$\alpha = -\beta \pm (2 + \beta^2)^{1/2}, \quad \beta = \tfrac{3}{2}(p_r q_r + p_i q_i)/(p_r q_i - p_i q_r), \tag{5}$$

$$\kappa^2 = \frac{-A\gamma}{q_i + (A/p_i)(\alpha p_i - \tfrac{3}{2}p_r)^2} > 0, \quad A = (p_r q_i - p_i q_r)/3\alpha|p|^2, \tag{6}$$

$$K = (\alpha - \tfrac{3}{2}p_r/p_i)\kappa, \quad v = -3|p|^2\kappa/p_i, \tag{7}$$

where A can be always taken negative so that $\kappa^2 > 0$ by the choice of an appropriate branch of α. Another interesting but implicit solution is obtained by the marginal-stability condition introduced by Dee and Langer[9] for a different problem. This condition says that small disturbances near the shock front neither grow nor decay in the frame moving with the shock and gives the shock speed v^* and the wave number of the pattern behind the shock K^* as

$$v^* = 2|p|K_m, \quad K_m = (-\gamma/p_i)^{1/2}, \tag{8}$$

$$K^* = [(q_i|p| \pm p_i|q|)/(p_r q_i - p_i q_r)]K_m, \tag{9}$$

where a branch of K^* should be chosen so that $|K^*| \leq K_m$. A qualitative form of $\tilde{\psi}$ can be obtained by the explicit solution (4) since, as we see later, values of v^* and K^* are close to those of the explicit solution for most values of parameters. (The precise form of $\tilde{\psi}$ is numerically obtained and will be published elsewhere.) Numerical integrations of Eq. (1) under localized initial conditions are performed by means of the Adams-Bashforth explicit scheme[10] with mesh sizes $\Delta t = 0.055$ and $\Delta x = 0.3$. As localized initial conditions, we take a hyperbolic secant type of disturbances with various amplitudes and widths and it is confirmed that our results are insensitive to such initial conditions except initial transitional phases. The accuracy of numerical experiments is checked by changing mesh sizes. As exhibited in Fig. 1, results of our numerical simulations show that definite values of speed and wave number (v^* and K^*) are selected according to the marginal stability condition when $p_r q_r + p_i q_i < 0$ or $p_r q_r + p_i q_i$ is positive but not close to 1. A typical propagation pattern is shown in Fig. 2(a), where $p_r q_r + p_i q_i = -3.2$ and $\psi(x,0) = \text{sech}(0.05x)$. It should be noted that the marginal-stability condition depends only on linear properties of the motionless state and all selected patterns in Fig. 1 are found to be unstable to modulational disturbances (see Stuart and DiPrima[11] for the modulational instability). Therefore, further transitions occur in the selected pattern. Since there exist stable longer-wavelength states than the selected one in the case $p_r q_r + p_i q_i < 0$, a stabilized longer-wavelength region follows after the selected pattern. However, the width of the stabilized region increases very slowly so that the selected shorter-wavelength pattern develops well and two distinct coherent patterns emerge with a sharp boundary in this case [Fig. 2(b)].

(2) The spatiotemporal transition to a chaotic state occurs in the case $p_r q_r + p_i q_i > 0$ where any finite-amplitude plane waves become unstable. When the modulational instability is not so strong that $p_r q_r + p_i q_i$ is positive but not close to 1, a periodic pattern still emerges behind the first shock front. As soon as the pattern selection occurs, a chaotic region develops in the selected pattern with a formation of the second front of a slower propagation speed as shown in Fig. 3(a). The propagation speed of the chaotic region is estimated by applying the marginal-stability analysis to the second front. Substituting $\psi = \rho^{1/2} \times \exp[i\{\int^x \sigma(x,t)\,dx - \Omega t\}]$ $[\rho(x,t) > 0]$ into Eq. (1) and linearizing the resulting equation around the selected plane wave as $\rho = \rho_0 + \delta\rho\, e^{i(kx-\omega t)}$, $\sigma = K^* + \delta\sigma\, e^{i(kx-\omega t)}$, where $\Omega = p_r K^{*2} - q_r \rho_0$, $\rho_0 = (\gamma + p_i K^{*2})/q_i$, we get the following dispersion re-

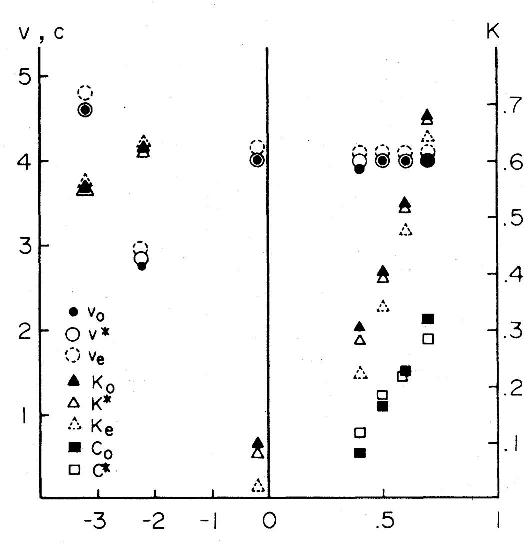

FIG. 1. Selected speed (v) and wave number (K) of periodic pattern vs various values of $p_r q_r + p_i q_i$: v_0, K_0, observed speed and wave number; v^*, K^*, theoretical speed and wave number given by Eqs. (8) and (9); v_e, K_e, speed and wave number of the explicit solution (4); c_0, observed speed of chaotic state; c^*, theoretical speed of chaotic state determined by Eqs. (10)–(12).

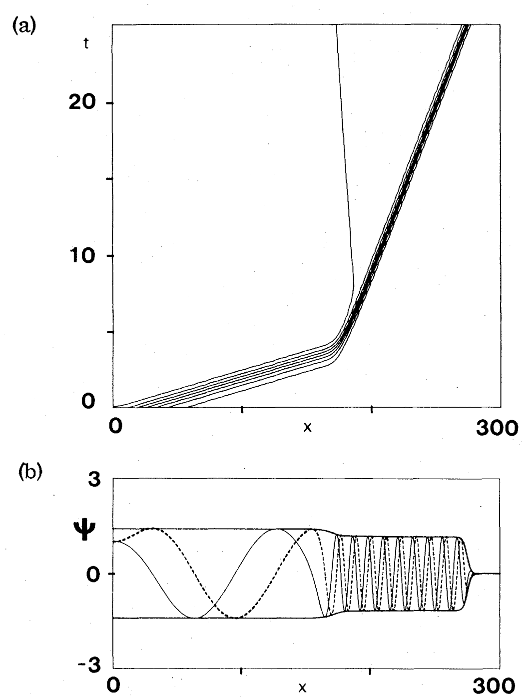

FIG. 2. Transition to periodic pattern for $p_r q_r = -1$, $p_i = -2.2$, $q_i = 1$, $\gamma = 2$ ($p_r q_r + p_i q_i = -3.2$) (a) Contours of equal $|\psi(x,t)|$ vs x and t; (b) spatial patterns for Reψ (solid curve) and Imψ (dotted curve) at $t = 25$.

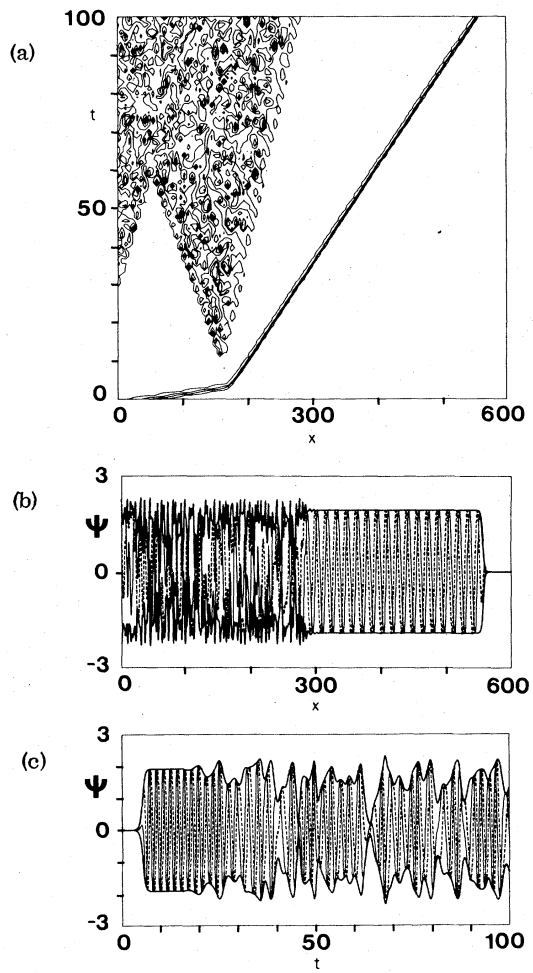

FIG. 3. Transition to chaotic state for $p_r q_r = 1$, $p_i = -1$, $q_i = 0.5$, $\gamma = 2$ ($p_r q_r + p_i q_i = 0.5$) (a) Contours of equal $|\psi(x,t)|$ vs x and t; (b) spatial patterns for Reψ (solid curve) and Imψ (dotted curve) at $t = 100$; (c) temporal transition to chaotic state at $x = 180$.

lation:

$$\tilde{\omega}^2 = W(k), \tag{10}$$

where $\tilde{\omega} = \omega - 2p_r k K^* + i(q_i \rho_0 - k^2 p_i)$ and

$$W(k) = -q_i^2 \rho_0^2 - 2p_r q_r \rho_0 k^2 + k^2(p_r^2 k^2 - 4p_i^2 K^{*2}) + 4ip_i kK^*(p_r k^2 - q_r \rho_0).$$

The stationary-phase and marginal-stability conditions in the moving frame with a constant velocity c^* give

$$2\tilde{\omega}(c^* - 2p_r K^* - 2ip_i k) = dW/dk, \tag{11}$$

$$\mathrm{Im}\,\omega = c^* \,\mathrm{Im}\, k. \tag{12}$$

The velocity c^* can be determined as a root of

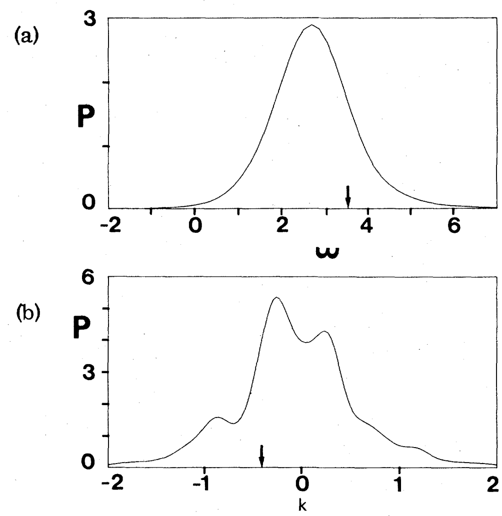

FIG. 4. Spatial and temporal power spectra of ψ in the chaotic region for parameters of Fig. 3. (a) Temporal power spectrum of ψ ($x = 180$, $t > 30$); (b) spatial power spectrum of ψ ($x < 300$, $t = 100$).

Eqs. (10)–(12) and numerically calculated values of c^* are found to agree approximately with observed speeds (see Fig. 1). In the examples in Fig. 1 propagation speeds of selected patterns are greater than those of the chaotic region and a coherent pattern coexists with a chaotic region. In other words, there occur the spatiotemporal transition from an unstable fixed point ($\psi = 0$) to a limit cycle (which produces a coherent spatial pattern) and the transition from the limit cycle to a chaotic state. Figures 3(b) and 3(c) show such spatial and temporal transitions, respectively. When the modulational instability becomes strong enough that $p_r q_r + p_i q_i$ is slightly smaller than 1 (note $|p_r q_r| = 1$, $p_i q_i < 0$), a coherent pattern disappears and a direct transition from $\psi = 0$ to a chaotic state occurs. Spatial and temporal power spectra of ψ in the chaotic region indicate that temporal development of ψ is as chaotic as spatial variation is, since the width of the temporal spectrum normalized by a peak frequency is the same order of magnitude as the normalized width of the spatial spectrum (Fig. 4). The peak frequency and wave number are slightly smaller than those of a selected periodic pattern, which are indicated by arrows in Fig. 4.

As concluding remarks, we should note the following points. The first result that a selected pattern is modulationally unstable is quite different from the previously discovered selected pattern[9] which is stable. This fact is essential to the subsequent transitions to a stabilized pattern or a chaotic state. Secondly, the transition to a chaotic state investigated here is a new type of transition to turbulence in the sense that the transition from a periodic pattern occurs spatially and temporally for fixed external parameters. This means the coexistence of a periodic pattern and a chaotic state for the same parameters. Previous studies[6,8] treated only the transition to turbulent motion associated with changing external parameters. Finally spatial inhomogeneities drive chaos in our model since the modulational instability is its origin and spatial chaos is as strong as temporal chaos. Such a chaotic state is in contrast with chaos in a perturbed sine-Gordon system where temporal chaos is dominant.[12]

We wish to thank Professor T. Taniuti for helpful discussions and Mr. S. Ishiguro for his help in the calculation of power spectra. Numerical simulations were performed by Facom M200 in the Institute of Plasma Physics, Nagoya University, Japan.

[1]H. Haken, *Synergetics, An Introduction* (Springer-Verlag, Berlin, 1978).

[2]A. C. Newell and J. A. Whitehead, J. Fluid Mech. 38, 279 (1969).

[3]S. Kogelman and R. C. DiPrima, Phys. Fluids 13, 1 (1970).

[4]K. Stewartson and J. T. Stuart, J. Fluid Mech. 48, 529 (1971).

[5]K. Katou, Nagoya University Report No. DPNU-83-08, 1983 (unpublished).

[6]Y. Kuramoto, Prog. Theor. Phys. 56, 679 (1976).

[7]N. Bekki, J. Phys. Soc. Jpn. 50, 659 (1981).

[8]H. T. Moon, P. Huerre, and L. G. Redekopp, Phys. Rev. Lett. 49, 458 (1982).

[9]G. Dee and J. S. Langer, Phys. Rev. Lett. 50, 383 (1983).

[10]S. A. Orszag and A. T. Patera, J. Fluid Mech. 128, 347 (1983).

[11]J. T. Stuart and R. C. DiPrima, Proc. Roy. Soc. London, Ser. A 362, 27 (1978).

[12]A. R. Bishop, K. Fesser, P. S. Lomdahl, W. C. Kerr, M. B. Williams, and S. E. Trullinger, Phys. Rev. Lett. 50, 1095 (1983).